Jour. Korea Inst. Mining Geol.
(1983) Vol. 16, No. 2, pp. 83-109

Petrology and Geochemistry of the Cretaceous Palgongsan Granite, Southern Korea.

Young Kook Hong*

Abstract: The Cretaceous Palgongsan granite is a typical, calc-alkaline, subsolvus monzogranite and shows characteristics of "I-type" granite by mineralogy and chemical composition. Many of the major and trace element characteristics of the Palgongsan granite are consistent with a relationship by fractional crystallisation to form a chemically zoned pattern.

The granite show light REE enrichment with (Ce/Yb)N ratios of 5.78–9.50. All the REE patterns show Eu negative anomalies which become larger from the margin (Eu/Eu* = 0.75) to the core (Eu/Eu* = 0.24) of the pluton, mainly due to feldspar fractionation. Mineral geochemistry (alkali-feldspar, plagioclase & biotite) studies also show the zonal structure of the Palgongsan granite. The two-feldspar geothermometer shows that the temperature difference between the margin and the core part of the pluton is about 200°C at various assumed pressures.

1. Introduction

The Cretaceous period in Korea was characterised by non-marine, terrestrial sedimentation, which was accompanied by volcanism in the Gyeongsang sedimentary basin (Jin et., al 1981). The sedimentation was terminated by the late Cretaceous climactic volcanism and granitic magmatism (Lee, 1974). The volcano–sedimentary pile is known as the Gyeongsang Supergroup (Chang, 1975), which is about 9,000m thick, and is divided into three Groups based on the volcanic constituents. The lower part of the Supergroup is exclusively composed of non-volcanic detritus, whilst the middle part is characterised by a mixture of nonvolcanic and volcanic sediments. The upper part consists predomanantly of pyroclastics and volcanic flows (Chang, op cit). The bulk of the Gyeongsang sedimentary sequence had been interpreted as fluvial or lacustrine deposits on the basis of sedimentary studies and fossils, except the lower part which indicates an alluvial fan origin(Choi, 1979). Such an interpretation is further supported by the pressence of some vascular plant fossils (Tateiwa, 1929) and remains of molluscs (Tateiwa op cit; Kobayashi & Suzuki, 1937; Yang, 1976, 1979), ostracods, and estherians indicating non–marine environments.

Igneous activity in the basin is divided into volcanism, plutonism and hypabyssal intrusion, most of which took place in the southern part of the basin. In composition, the pyroclastics generally range form rhyolitic to dacitic, whereas volcaniclastics and flows range from rhyolitic to andesitic compositions. Following the volcanism, plutonism occurred generally along the weak zones in a NNE direction as batholiths and smaller scattered plutons in oval or elliptical shapes. The plutonic rocks show a range from diorite and quartz diorite, through granodiorite and granite to alkali–feldspar granite (Jin et al., 1981).

The Cretaceous Palgongsan granite is located in the NW part of the Gyeongsang sedimentary basin, and is expose over an area of approximately 240 square kilometres (24Km x 10Km); it has an oval shape in plan and is moderately elongated in a N60°W direction. The highest peak in the studied area is Mt. Palgong which is 1,192 metres above sea level. The accompanying stratigraphic and sample location map (Fig. 1) shows the geology surrounding the sampled section of the Cretaceous Palgongsan granite. The studied area

*Geochemical Exploration Division, Korea Institute of Energy and Resources (KIER)

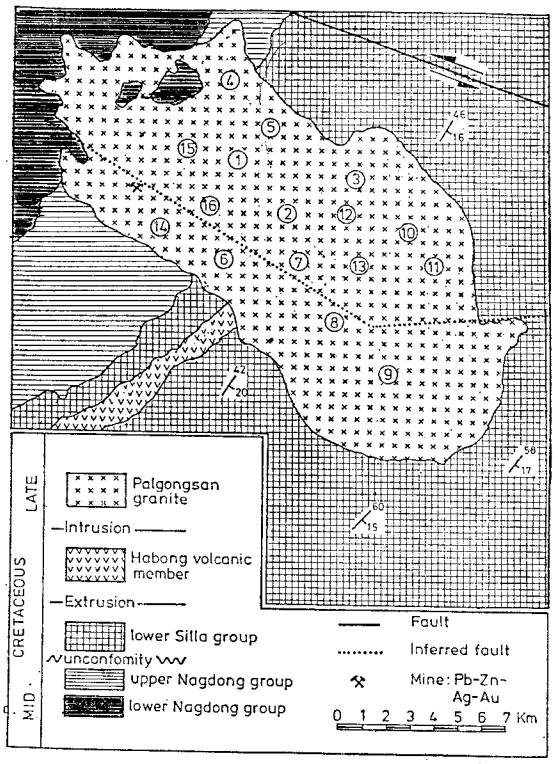

Fig. 1 Stratigraphy and sample location map of the Cretaceous Palgongsan granite. (Tateiwa, 1929).

was previously mapped at 1:50,000 scale by Tateiwa (1929), and at 1:250,000 scale by the Geological and Mineral Institute of Korea (1973). The age of the Palgongsan granite has been radiometrically dated as 73 m. y. by K/Ar method on potassium feldspars (Kim, 1971).

2. Field relations

The sedimentary rock types of the Gyeongsang Supergroup in the studied area (Fig. 1.) consist of the lower Nagdong Group, upper Nagdong Group and lower Silla Group (Chang, 1978). The lower Nagdong group, which is distributed in the NW marginal part of the studied area, is composed of dark to light grey sandstone, shale, mudstone, arkosic sandstone, conglomerate, coaly shale and purple shale. The upper Nagdong Group is characterised by dark to light grey sandstome, shale, mudstone and black shale, brown conglomerate, purple tuffaceous sandstone, and purple shale. The lower Silla Group, which is distributed at the SE part of the area, consists of brown and purple conglomerate, sandstone, and shale.

In general, the sedimentary rock show N40°–60°E strike and 15°–30° SE dip directions. The Hagbong volcanic member (see stratigraphy in Fig. 1) was extruded upon the sedimentary rocks; it mainly consists of tuffaceous andesitic rocks interbedded with the sedimentary rocks.

The contact between the Palgongsan granite and the country rock is sharp and steeply inclined. The contact zones are thermally metamorphosed to hornfels, which range about 1–1.5Km in width from the granite body. The Palgongsan granite is generally a medium grained porphyritic granite which is composed of quartz, feldspars, biotite, and hornblende. The grain size of the granite increases form the marginal to the central part of the pluton; fine grained (equigranular) biotite rich granite with intermediate volcanic xenoliths occur at the margin, whereas the central part of the pluton is medium grained and xenolith-free. Finer-grained margins of plutonic bodies have traditionally been considered to result from chilling. The fine grain size results from loss of heat to the wall rocks, which causes temperatures to fall more rapidly in the marginal part of the magma than in the interior, promoting the formation of abundant new nuclei and shortening their growth time and, consequently, their size before they solidify to form the marginal rocks. Intermediate xenoliths and tourmaline veins are numerous at the margin. The rounded shape of the xenoliths implies that the xenoliths are digested by granitic melt.

The principal ore minerals in the Chilgog mine, which is located in NW of the Palgonsan granite (see Fig. 1), are Au, Ag, Pb and Zn-bearing.

The mineralisation is controlled by the structures such as fissures, cracks and faults parallel with N40°W strike and 75°–85°NE dipping joints. The most dominant joint direction of the Cretaceous Palgongsan granite is N50°–70°W, which is generally parallel to the faults and elongation of the pluton (and at right angles to the Sinian direction).

3. Petrography

Quartz (about 30%; see Table 1.) has sutured–boundaries and occurs as anhedral crystals with 1.5–2mm average length in the central part of the Palgongsan granite, and clustered aggregates fine–grained (0.5–1mm in length) in the margin. Micrographic intergrowth between quartz and alkali–feldspar is common and the quartz grains fill interstices between alkali–feldspar and plagioclase crystals. Poikilitic quartz, with inclusions of plagioclase and biotite, is seen over the whole area. The quartz shows normal extinction, and particularly quartz is slightly fractured in the contact area.

Alkali–feldspar (about 35%; Table 1) is up to 4mm in length with an average of 1.5mm. Microperthite is dominant and consists mostly of the irregular string–type. The alkali–feldspar occurs interstitially and shows graphic intergrowth with quartz. Poikilitic alkali–feldspar with inclusions of biotite, quartz and magnetite is commonly observed. Some of the alkali–feldspars are slightly altered to sericite.

Plagioclase crystals (about 30%; Table 1) occur in subhedral, columnar plates which show parallel twinning. The early crystallised euhedral plagioclase is often overgrown by oscillatory zoned plagioclase, which is predominantly observed in the mid–central part of the pluton. The length of plagioclase is up to 2.5mm with an average of 1mm in grain size. The plagioclase is identified by Michel–Lévy method as oligoclase (An 12–16) and is slightly altered to sericite. Alteration attacks the centres of the plagioclase, leaving relatively unaltered margins.

Biotite (about 3%; Table 1) occurs as subhedral discrete flakes which range up to 1mm in length with an average of 0.5mm. Poikilitic biotites are observed with inclusions of zircon, apatite and magnetite. Biotite is predominantly brownish–green in plane light. Biotite, form the marginal part of the pluton, is observed to be dark grey–green instead, and often encloses some zircons, which may be due to high Mg/(Mg+Fe) in biotite. Some of the biotites are slightly altered to chlorite.

The principal accessory minerals are apatite, zircon, magnetite, horblende and tourmaline. Apatite occurs as irregular needle–shape acicular crystals which are mostly included in biotite and rarely in plagioclase. Zircon, which is up to 0.1mm in length, is observed as inclusions within biotite crystals. Magnetite occurs as subhedral grains with up to 0.5mm in lenght, which are frequently distributed in and around biotite. Hornblende is often fringed by biotite. Hornblende shows subhedral grains which are mostly abundant in the chilled margin of the pluton. The size of hornblende is up to 1.5mm in length with an average of 0.4mm. Feldspars and biotite overgrow the hornblende. Tourmaline is one of the last minerals to crystallise, and is overgrown on the biottie.

4. Modal analysis

Modal analysis of the minerals present in each specimen from the Palgongsan pluton was carried out from etched and stained thin sections. The details of modal compositions are presented in Table 1. Only alkali–feldspars were stained using the sodium cobaltinitrate method (Bailey & Stevens, 1960). Most samples were counted for 2,000 equally spaced points. All Palgongsan granites plot in the monzogranite region, according to Streckeisen's classification (Fig. 2). Mafic minerals are generally abundant at the marginal

Table 1. Modal composition of the Cretaceous Palgongsan granite

	CP. 1	CP. 2	CP. 3	CP. 4	CP. 5	CP. 6	CP. 7	CP. 8	CP 9	CP 10	CP. 11	CP. 12	CP. 13	CP. 14	CP. 15	CP. 16
Quartz	31.3	32.1	36.8	26.2	25.7	25.4	34.1	35.3	27.8	26.3	37.0	40.2	34.0	26.7	28.3	29.3
K-feldspar	33.5	29.3	37.8	33.9	35.9	32.4	24.9	31.7	42.1	49.7	28.3	37.2	24,7	45.7	28.0	25.8
Plagioclase	32.7	33.1	22.9	33.9	33.5	37.3	35.4	30.0	27.0	30.2	28.6	21.8	37.5	27.6	35.6	40.4
Biotite	1.5	3.1	2.3	4.0	2.5	3.5	4.7	2.3	1.6	2.8	5.2	0.8	1.7	6.4	5.3	3.0
Tourmaline	—	—	—	—	0.1	—	—	—	—	0.1	—	—	—	—	—	—
Hornblende	0.2	0.3	—	1.2	1.5	0.5	—	—	0.8	0.3	—	—	0.4	—	2.5	0.5
Zircon	—	0.1	—	—	—	—	—	—	—	0.2	0.2	—	0.2	—	—	0.2
Apatite	0.3	0.2	—	—	—	0.2	0.1	—	—	—	—	—	—	—	—	0.1
Opaques	0.5	1.8	0.2	0.8	0.8	0.7	0.8	0.7	0.7	0.4	0.7	—	1.5	—	0.3	0.7
Qz+AF	65.0	61.5	74.6	60.1	61.6	57.9	59.1	67.0	69.9	66.0	65.3	77.4	58.7	72.4	56.3	55.2
PL	32.8	33.2	22.9	33.9	33.5	37.4	35.4	30.0	27.0	30.2	28.6	21.8	37.5	27.6	35.6	40.4
Mafics	2.2	5.3	2.5	6.0	4.9	4.7	5.5	3.0	3.1	3.8	6.1	0.8	3.8	6.4	8.1	4.4

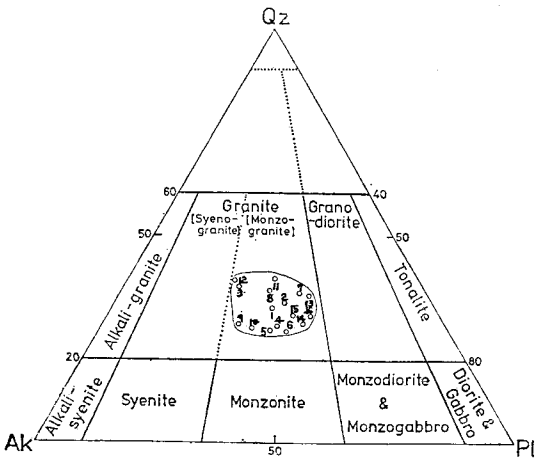

Fig. 2 Distribution of rock types in the Palgongsan pluton using the modal classification of Streckeisen (1976)

part relative to the centre of the pluton. In contrast, the abundance of quartz and alkali-feldspar increases from the chilled margin inward.

The progressive change in the compositional range throughout the Palgongsan pluton clearly indicates that differentiation in the sequence results from crystal fractionation. The simplest comagmatic plutonic sequence is a concentrically zoned pluton such as the Palgongsan granite, in which relatively mafic rock in the margins, composed of high temperature mineral assemblages, passes inward without discontinuities to more felsic rock in the core, composed of lower temperature mineral assemblages, which is similar to the Galloway plutons in the south of Scotland (Stephens & Halliday, 1979). This modal compositional pattern indicates that this pluton solidified from its margins inwards with falling temperature.

5. Mineral paragenesis

The finer margin and medium grain in the central part of the Plagongsan granite suggests that solidification started from the margin and progressed inward. The sequence of crystallisation appears to be from early precipitation of accessories to the probobly simultaneous nucleation of hornblende and plagioclase. Increasing sodic content of plagioclase was accompanied by biotite crystallisation, and the last minerals to crystallise are those with interstitial habits, such as alkali-feldspar and quartz. In the pneumatolytic stage of alteration, tourmaline occurred by the introduction of boron which had attacked the granitic minerals, mainly biotite and feldspar.

For a consideration of the results taken from field and petrographic work on the Palgongsan granite, the following local conclusions are tentatively drawn:

1) The grain size of the granite increases from

Table 2. Major oxide element analyses and CIPM Norms of the Cretaceous Palgongsan granite

	CP. 1	CP. 2	CP. 3	CP. 4	CP. 5	CP. 6	CP. 7	CP. 8
SiO_2	70.50	70.92	72.10	68.52	68.88	69.38	71.40	71.00
TiO_2	0.35	0.31	0.29	0.41	0.46	0.34	0.33	0.33
Al_2O_3	14.47	14.71	13.84	14.32	14.94	14.49	14.59	14.22
Fe_2O_3	1.63	1.92	1.45	2.10	2.11	1.94	1.50	1.84
FeO	2.02	2.28	1.85	2.99	2.51	2.56	1.88	2.02
MnO	0.10	0.12	0.05	0.09	0.10	0.11	0.10	0.12
MgO	0.72	0.57	0.63	0.96	1.04	0.65	0.60	0.67
CaO	2.23	1.72	1.67	2.26	2.38	1.71	1.72	1.70
Na_2O	4.22	3.57	3.42	3.90	4.06	4.01	4.08	4.13
K_2O	3.65	4.09	4.52	3.90	3.89	4.01	4.11	4.23
P_2O_5	0.11	0.09	0.08	0.13	0.15	0.10	0.10	0.10
Total	100.01	100.30	99.92	99.56	100.52	99.31	100.41	100.37
CIPW Norms								
Qz	25.67	29.17	29.79	23.59	23.11	25.11	26.80	25.58
Or	21.57	24.17	26.71	23.05	22.99	23.70	24.29	25.00
Ab	35.71	30.21	28.94	33.00	34.36	33.93	34.52	34.95
An	9.76	7.95	7.76	10.05	10.83	7.83	7.88	7.77
Di	0.49	—	—	0.26	—	—	—	0.01
Hy	3.52	3.73	3.38	5.51	4.88	4.36	3.35	3.53
Mt	2.36	2.78	2.10	3.04	3.06	2.81	2.17	2.67
Cr	—	1.50	0.48	—	0.08	0.68	0.54	—
Il	0.67	0.59	0.55	0.78	0.87	0.65	0.63	0.63
Ap	0.26	0.21	0.19	0.30	0.35	0.23	0.23	0.23
K_2O/Na_2O	0.86	1.15	1.32	1.00	0.96	1.00	1.01	1.02
$Al_2O_3/(K_2O+Na_2O)$	1.84	1.92	1.74	1.84	1.88	1.81	1.78	1.70
$K_2O/(K_2O+Na_2O)$	0.46	0.53	0.57	0.50	0.49	0.50	0.50	0.51
$CaO/(K_2O+Na_2O)$	0.28	0.22	0.21	0.29	0.30	0.21	0.21	0.20
FeO(t)/MgO	5.07	7.37	5.24	5.30	4.44	6.92	5.63	5.76
L. I.	22.18	23.16	24.40	20.53	20.92	22.22	23.71	23.51
D. I.	82.95	83.55	85.44	79.64	80.45	82.74	85.61	85.53
FeO/Fe_2O_3	1.24	1.19	1.28	1.42	1.19	1.32	1.25	1.10

L. I. : Larsen Index
D. I. : Differentiation Index

the marginal (mafic) to central (leucocratic) part of the pluton.

2) The joint patterns (N50°–70°W dominant), consistent with a fault system (and elongation of the pluton), developed by compression. The structural relation between the granite intrusion and its joint patterns suggests that during intrusion the roof of the granite broke into rectangular blocks along previously established lines of weaknesses, such as joints and vertical faults, in the country rock. However, there are no penetrative linear or planar structures in the Palgongsan granite.

3) From margin to interior all show a decrease in mafic minerals matched by a proportional incresed in alkli-feldspar and quartz. The

Table 2. (continued)

	CP. 9	CP. 10	CP. 11	CP. 12	CP. 13	CP. 14	CP. 15	CP. 16
SiO_2	70.11	71.33	70.01	75.55	70.10	67.53	69.38	69.04
TiO_2	0.32	0.32	0.36	0.12	0.32	0.49	0.41	0.35
Al_2O_3	15.29	14.40	14.55	12.35	14.08	14.96	14.48	15.00
Fe_2O_3	1.55	1.52	1.74	1.12	2.01	1.91	1.75	1.92
FeO	2.27	2.05	2.29	1.32	2.34	2.75	2.77	2.42
MnO	0.07	0.08	0.09	0.06	0.16	0.09	0.06	0.12
MgO	0.61	0.55	0.71	0.13	0.54	1.31	0.88	0.79
CaO	1.71	1.68	1.82	0.45	1.53	2.79	2.37	1.87
Na_2O	4.08	4.14	4.28	3.46	4.05	3.93	3.62	4.08
K_2O	4.17	4.15	3.86	4.94	4.33	3.61	4.23	3.95
P_2O_5	0.10	0.11	0.11	0.03	0.10	0.16	0.13	0.11
Total	100.26	100.33	99.88	99.52	99.56	99.53	100.08	99.66
CIPW Norms								
Qz	25.00	26.29	24.63	34.80	25.08	22.15	24.74	24.18
Or	24.64	24.52	22.81	29.19	25.59	21.33	25.00	23.34
Ab	34.52	35.03	36.22	29.28	34.27	33.26	30.63	34.52
An	7.83	7.62	8.31	2.04	6.94	10.77	10.77	8.56
Di	—	—	—	—	—	0.23	0.12	—
Hy	4.01	3.50	4.11	1.74	3.75	5.98	5.21	4.47
Mt	2.25	2.20	2.52	1.62	2.91	2.77	2.54	2.78
Cr	1.20	0.31	0.29	0.57	0.19	—	—	0.88
Il	0.61	0.61	0.68	0.23	0.61	0.93	0.78	0.67
Ap	0.23	0.26	0.26	0.07	0.23	0.37	0.30	0.26
K_2O/Na_2O	1.02	1.00	0.90	1.43	1.07	0.92	1.17	0.97
$Al_2O_3/(K_2O+Na_2O)$	1.85	1.74	1.79	1.47	1.68	1.98	1.84	1.87
$K_2O/(K_2O+Na_2O)$	0.51	0.50	0.47	0.59	0.52	0.48	0.54	0.49
$CaO/(K_2O+Na_2O)$	0.21	0.20	0.22	0.05	0.18	0.37	0.30	0.23
FeO(t)/MgO	6.26	6.49	5.68	18.77	8.06	3.56	5.14	5.49
L. I.	22.95	23.65	22.38	28.22	23.29	19.27	21.34	21.88
D.I.	84.16	85.84	83.66	93.27	84.93	76.73	80.37	82.04
Fe/Fe_2O_3	1.46	1.35	1.32	1.18	1.16	1.44	1.58	1.26

progressive change in the compositional range in the pluton indicates that differentiation in the sequence results from crystal fractionation. Quartz crystals occur interstitially and show graphic texture. The oval shape and mineral texture of the pluton suggest high crustal level granite.

4) All the Palgongsan granite plot in the monzogranite region(Streckeisen, 1976) and belong to the "magnetite" series (Ishihara, 1977).

6. Whole rock geochemistry

The whole rock geochemistry study is based upon the analyses of 16 representative granite samples. The localities of the analysed samples are shown in Fig. 1. Bulk rock major oxide elements were analysed by the X-ray fluorescence spectometry (XRF) method on fused glass discs. FeO was measured by the wet analysis using the method of Wilson (1955), and Fe_2O_3 was obtained

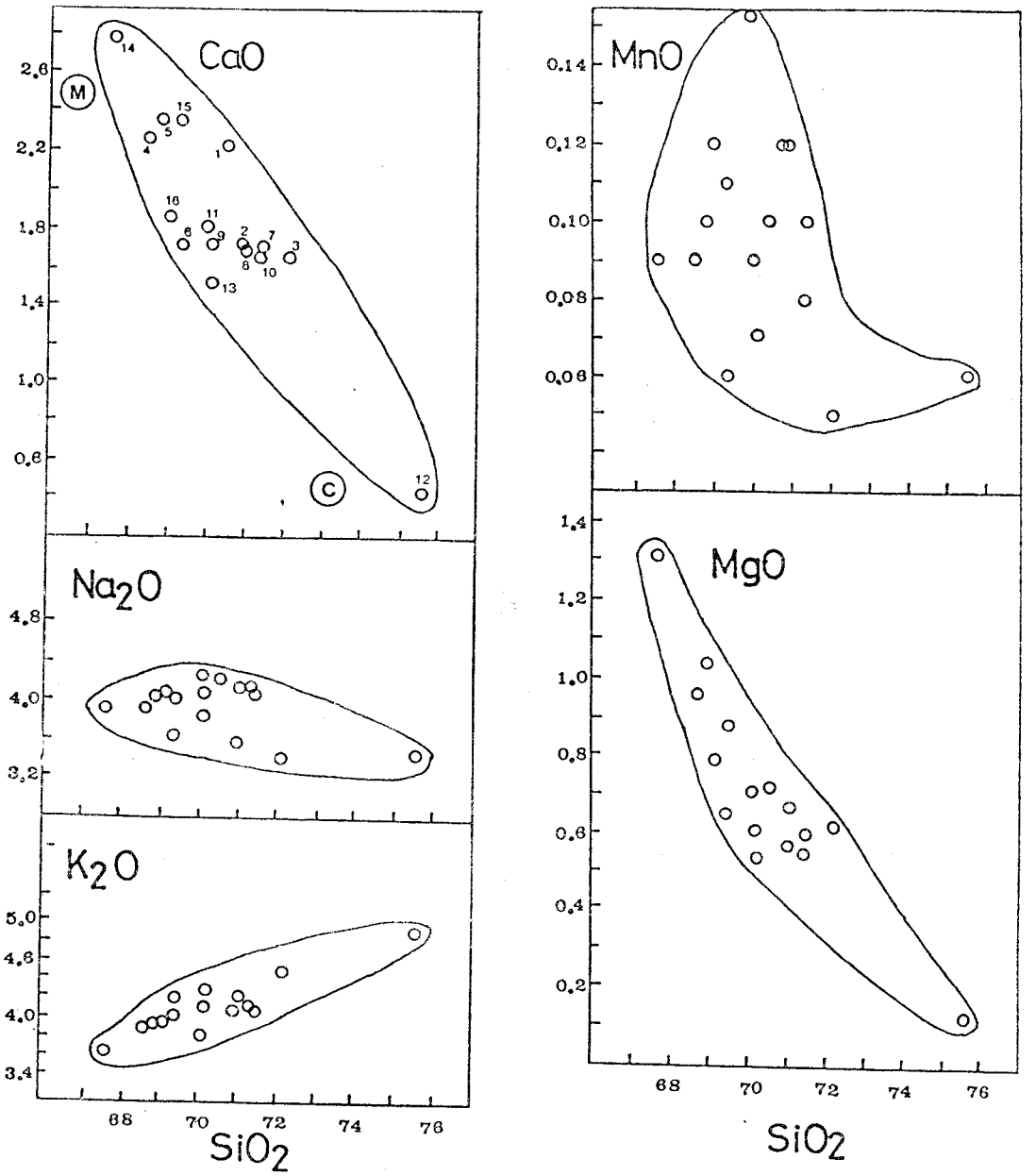

Fig. 3 Harker (major elements in wt. %) Variation diagrams for the analysed samples of the Cretaceous Palgongsan granite.
(M : margin of the pluton
C : core of the pluton

by XRF determined total iron-(FeO×1.1113). Trace elements were also determined by XRF analysis on pressed powder pellets. The concentration of the rare-earth elements (REE) were obtained by instrumental neuton activation analysis (INAA). Details of sample preparation, anlytical methods, their accuracy and precision can be sent by the authour upon request. No previously published work on the geochemistry of the Palgongsan granite is available.

6. 1 Major elements chemistry

The analytical results of 11 major oxide elements

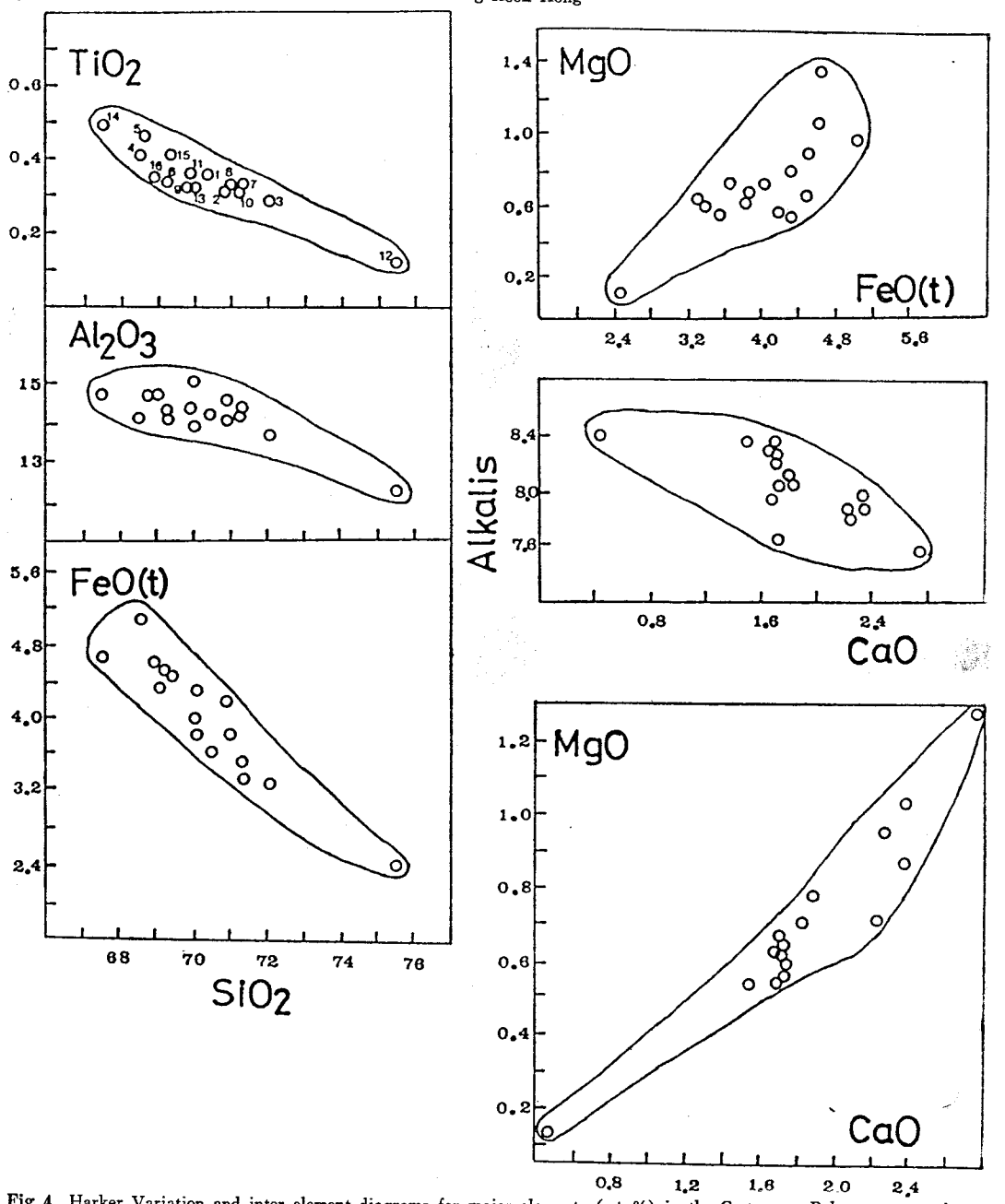

Fig. 4 Harker Variation and inter-element diagrams for major elements (wt. %) in the Cretaceous Palgongsan granite.

and CIPW norms are presented in Table 2. The variation in chemical composition is demonstrated clearly in Harker diagrams (Fig. 3 and Fig. 4). Differentiation Index (Thornton & Tuttle, 1960) and Larsen Index (Larsen, 1948) are also shown in Table 2. Differentiation in terms of the widely used AFM and NCK diagrams is shown in Fig. 5a and Fig. 5b, respectively.

The silica content of analysed samples for the Palgongsan granite ranges from 67.53 wt% to 75.55 wt%: arithmetical mean ($\bar{x}$) and sample standard diviation (S) are 70.36 wt% and 1.83 wt%, respectively. Silica content increases from the marginal to the central part of the pluton.

The plots of K_2O against SiO_2 appear to show a positive trend in the Palgongsan granite (Fig. 3). The K_2O content varies from 3.61 wt% to 4.94 wt%(average value of 4.1±0.33 wt%). The K_2O content generally increases from the chilled margin to the central part of the pluton. The correlation between Na_2O a nd SiO_2 in the studied area show little variation (Fig. 3). The concentration of Na_2O ranges from 3.42 wt% to 4.28 wt% (mean value of 3.94±0.27 wt%). The ratio of K_2O/Na_2O (see Table 2) is generally about 1.0 and increases from the margin inward. The total alkalies (K_2O+Na_2O) show that the concentration increases generally form margin to core of the pluton. Total alkali contents are plotted against CaO in Fig. 1.4, which illustrates a negative correlation. $CaO/(K_2O+Na_2O)$ ratio (mean value: 0.23±0.07) decreases from margin to inward of the Palgongsan granite (0.37 to 0.05). The manganese content ranges from 0.05 wt% to 0.16 wt% with a mean value of 0.1 ± 0.03 wt%. The distribution pattern of MnO shows a slight negative variation with SiO_2 (Fig. 3). The magnesium content of the studied pluton ranges widely from 0.13 wt% to 1.31 wt% (average value of 0.71 ± 0.26 wt%). The plot of MgO against SiO_2 shows a strong negative correlation (Fig. 3).

The concentration of MgO generally decreases from the marginal to the central part of the pluton. The content of total iron ranges from 2.44 wt% to 5.09 wt% (mean walue of 4.02 wt%). The plot of total iron versus SiO_2 shows a negative relationship (Fig. 4). The total iron concentrations decrease from margin to centre part of the pluton. The plots of MgO against total iron, and MgO versus CaO show positive trends (Fig. 4). The variation of the ratio of FeO/Fe_2O_3 in the pluton appears to be 1.3 ± 0.13. $(FeO+Fe_2O_3)$/ MgO ratios increases from margin (3.56) and inwards (18.77) in the Palgongsan granite. The content of TiO_2 ranges from 0.12 wt% to 0.49 wt% with a mean value of 0.34 ± 0.08 wt%. TiO_2 versus SiO_2 shows a negative correlation (Fig. 4). The content of TiO_2 generally decreases from the margin to the core of the pluton.

The concentrations of Al_2O_3 rangefrom 12.35 wt% to 15.29 wt% (mean value of 14.42 ± 0.66 wt%). The absolute amount of Al_2O_3 decreases slightly with increasing SiO_2 (Fig. 4). $Al_2O_3/(K_2O + Na_2O)$ decreases from margin (1.98) to centre (1.47) of the granite.

The content of calcium for the Palgongsan granite ranges from 0.45 wt% to 2.79 wt% with an average value of 1.85 ± 0.51 wt%. Plagioclase and apatitie are the main carriers for the calcium, the modal proportion of the minerals increasing from the centre to the marginal part of the pluton (see Table 1).

CaO is plotted against SiO_2 and alkalies in Fig. 3 and Fig. 4, respectively, which show negative correlations. Phosphorous contents are between 0.03 wt% and 0.16 wt% (mean value of 0.11 ± 0.03 wt%) and generally decrease from margin to centre of the pluton.

Differentiation and Larsen indices show that the indices continually increase from the margin to the centre part of the pluton. Many of the major element characteristics of the Palgongsan granite are consistent with a relationship by fractional crystallisation form its margins inward with falling temperature.

AFM and NCK ternary diagrams

The major element data from the Cretaceous Palgongsan granite, when plotted on the AFM diagram (Fig. 5a) define an enrichment trend typical of calc-alkaline series as presented by Petro et al. (1979). Plotting the alkalinity ratio of Wright (1969) versus SiO_2 shows that the Palgongsan granite plots within the calc-alkaline field, although some of the most siliceous (core part of the pluton) rocks fall in the alkaline field. Palgongsan granite shows more alkalies and less

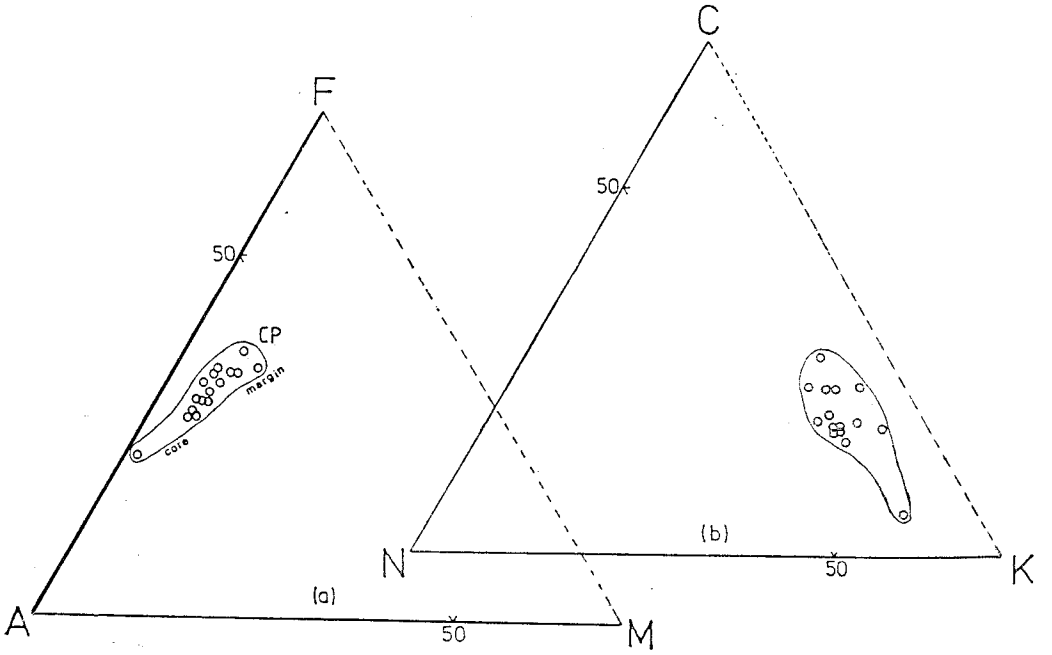

Fig. 5 AFM and NCK variation diagrams of the Cretaceous Palgongsan granite, with A=Na_2O+K_2O, F=FeO+Fe_2O_3, M=MgO, N=Na_2O, C=CaO, and K=K_2O in weight percent.

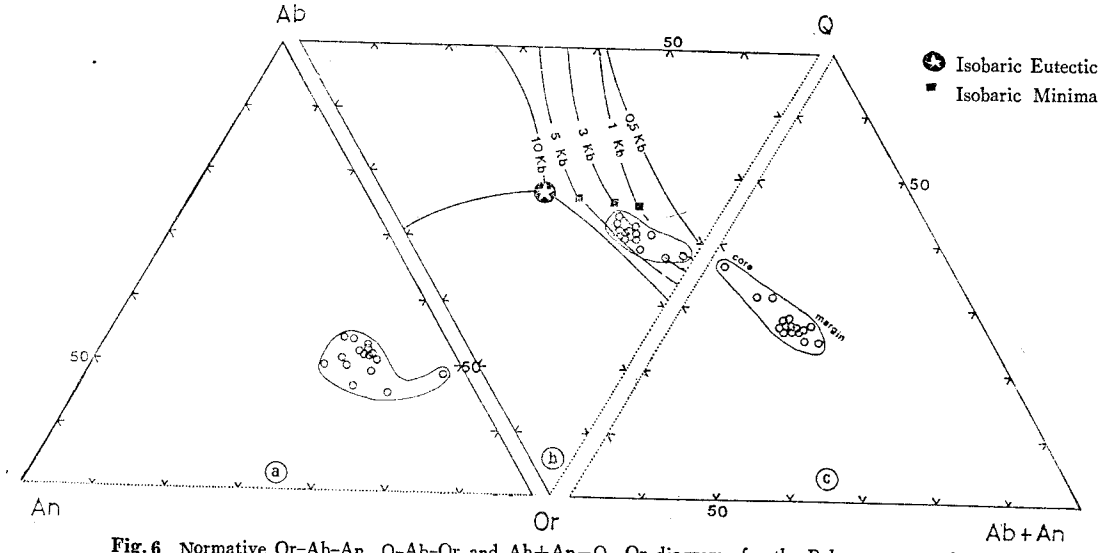

Fig. 6 Normative Or-Ab-An, Q-Ab-Or and Ab+An−Q−Or diagrams for the Palgongsan granite.

total iron contents from margin to central part of the pluton. The AFM diagram illustrates a typical single magma series which underwent fractionation of plagioclase and mafic minerals. Differentiation is also indicated by the NCK diagram (Fig. 5b) which confirms fractionation of a single magma. The trend shown in Fig. 5b is a consequence of the precipitation of more sodic plagioclase towards the end of the crystallisation sequence.

CIPW normative compositions and phase equilibria

The CIPW norm compositions are widely used for the silicic rocks (Chayes & Metais, 1963). The

Table 3. Trace elements analyses (in ppm) of the Cretaceous Palgongsan granite, arithmetical mean ($\bar{X}$) and sample standard deviation (S)

	CP. 1	CP. 2	CP. 3	CP. 4	CP. 5	CP. 6	CP. 7	CP. 8	CP. 9
Ni	3	4	3	5	3	5	1	3	3
Cr	8	10	7	15	8	14	4	7	7
Y	20	22	23	25	24	25	30	23	23
V	24	22	26	40	44	25	19	21	21
Zr	185	201	137	190	194	192	193	196	194
Nb	12	15	11	14	8	11	14	11	12
Rb	122	133	150	118	128	132	137	134	128
Sr	233	209	202	252	259	209	214	206	201
Th	12	15	17	14	13	13	17	15	10
K (X 1000)	30.30	33.95	37.52	32.37	32.29	33.28	34.11	35.11	34.61
Ca (X 1000)	15.93	12.29	11.94	16.15	17.01	12.22	12.29	12.15	12.22
Ti	2098	1858	1739	2458	2758	2038	1978	1978	1918
P	480.04	392.76	349.12	567.32	654.6	436.4	436.4	436.4	436.4
K/Rb	248	255	250	274	252	252	249	262	270
Rb/Sr	0.52	0.64	0.74	0.47	0.49	0.63	0.64	0.65	0.64
Ca/Y	797	559	519	646	709	489	410	528	531
Th/Nb	1.0	1.0	1.55	1.0	1.63	1.18	1.21	1.36	1.17
Nb/Y	0.60	0.68	0.48	0.56	0.33	0.44	0.47	0.48	0.52
K/Zr	164	169	274	170	166	173	177	179	178
Zr/Y	9.25	9.14	5.96	7.60	8.08	7.68	6.43	8.52	8.43
Ti/Zr	11.3	9.2	12.7	12.9	14.2	10.6	10.2	10.1	9.9

	CP. 10	CP. 11	CP. 12	CP. 13	CP. 14	CP. 15	CP. 16	$\bar{X}$	S
Ni	3	3	5	3	5	4	4	3.5	1.0
Cr	5	7	8	7	12	8	9	8.5	3.0
Y	21	26	31	23	27	22	27	24.3	3.5
V	20	28	ND	20	37	19	20	24	10
Zr	209	206	108	182	188	195	195	185	26
Nb	13	16	18	12	10	12	11	12.8	2.4
Rb	130	127	198	142	115	120	122	134	19
Sr	210	220	114	202	291	304	219	222	43
Th	14	18	26	10	12	17	14	15	4
K (X 1000)	34.45	32.04	41.00	35.94	29.96	35.11	32.79	34.05	2.70
Ca (X 1000)	12.01	13.01	13.22	10.93	19.94	19.94	13.36	13.23	3.67
Ti	1918	2158	719	1918	2938	2458	2098	2064	490
P	480.04	480.04	130.92	436.40	698.24	567.32	480.04	466	128
K/Rb	265	252	207	253	261	293	269	257	18
Rb/Sr	0.62	0.58	1.74	0.70	0.40	0.40	0.56	0.65	0.31
Ca/Y	706	500	105	475	739	770	495	561	171
Th/Nb	1.08	1.13	1.78	0.83	1.20	1.42	1.27	1.24	0.26
Nb/Y	0.76	0.62	0.58	0.52	0.52	0.55	0.41	0.53	0.10
K/Zr	165	156	380	197	159	180	168	191	57
Zr/Y	9.95	7.92	3.48	7.91	6.96	8.86	7.22	7.71	1.54

Ti/Zr	9.2	10.5	6.7	10.5	15.6	12.6	10.8	11.1	2.1

ND: None-detected

details for calculation of the CIPW norm is presented in Cox et al. (1979). Granites of the studied area with the sum of normative albite, orthoclase and quartz over 80% (Tuttle & Bowen, 1958), have been plotted (Fig. 6). Its phase characterstics are well known, with a thermal minimum between the alkali-feldspar solid solution series and quartz. Phase boundary curves for selected water-vapour pressures, and ternary minima for the respective phase boundary curves, are superimposed on the diagram in Fig. 6. Although the composition field of the Palgongsan granite forms a generally scattered pattern, the plot of Q-Ab-Or implies a PH_2O of about 2 kbars in the central part, and 4 kbars in most of the marginal part of the pluton. The phase relationships in the Or-Ab-An ternary feldspar system (Fig. 6) were first suggested by Tuttle & Bowen (op cit). The temperature distribution other the system shows a gradual decrease from the An apex toward a thermal trough between Or and Ab, which illustrates that the temperature of crystallisation gradually decreases from the margin to the central part of the Palgongsan granite. Normative Q-Or-(Ab+An) compositions are plotted with a good linear trend in Fig. 6. The abundance of plagioclase decreases continuously from the margin (An 16) to the centre (An 12) of the pluton.

6. 2 Trace and rare-earth elements chemistry

Trace and rare-earth element determinations for the 16 Palgongsan granite samples are presented in Table 3 and Table 4, respectively. The incompatible elements (i.e. those with bulk distribution coefficient, D, less than 1) have been broadly grouped according to their ionic radius/charge ratios, because their chemical behaviour is strongly dependent upon the mineralogy, pressure, temperature and initial liquid composition of the system under consideration. Thus, Rb, K, Sr, Th and U, which have low field strength ionic states, have been termed large ion lithophile (LIL) elements (Schilling, 1973), and Ti, P, Zr, Hf, Nb and Ta which have low radius/charge ratios have been termed high field strength (HFS) elements. The rare-earth elements (REE) and Y appear to occupy an intermediate position; therefore, Ce and La have been grouped with the LIL elements, and the remaining REE and Y with the HFS elements. The compatible elements, such as Ni, Cr and V, are grouped separately.

LIL elements, Ce, and La

Rb contents in the Palgongsan granite range from 115ppm to 198ppm with mean value of 134± 19ppm. Rb contents are plotted against SiO_2, which shows a positive correlation (Fig. 7). The concentrations of Rb increase from the centre of the pluton (Fig. 7). Sr contents range from 114ppm to 304ppm (average value of 222 ± 43ppm), which show a negative relationship with SiO_2 (Fig. 7). Sr consistently decreases because of early and continued plagioclase crystallisation. The plot of Sr against CaO shows a positive trend (Fig. 9). Rb/Sr ratios are generally higher in the centre (1.74) than in the chilled margin (0.40), with a mean value of 0.65 ± 0.31. plot between Rb/Sr and SiO_2 shows a positive trend (Fig. 7). K/ Rb ratios generally decrease from the margins (270-293) inward (207) in the pluton with a mean ration of 257 ± 18 (Fig. 7). The K/Rb ratio is affected by crystallisation of alkli-feldspar and biotite, which is also illustrated in the modal composition (Table 1). For the K/Rb ratio, if neither an alkali-feldapar nor a biotite-phlogopite is present in the residue, it is difficult to reduce the K/Rb ratio of the melt relative to the parent by the factor of differentiation (Hanson, 1978).

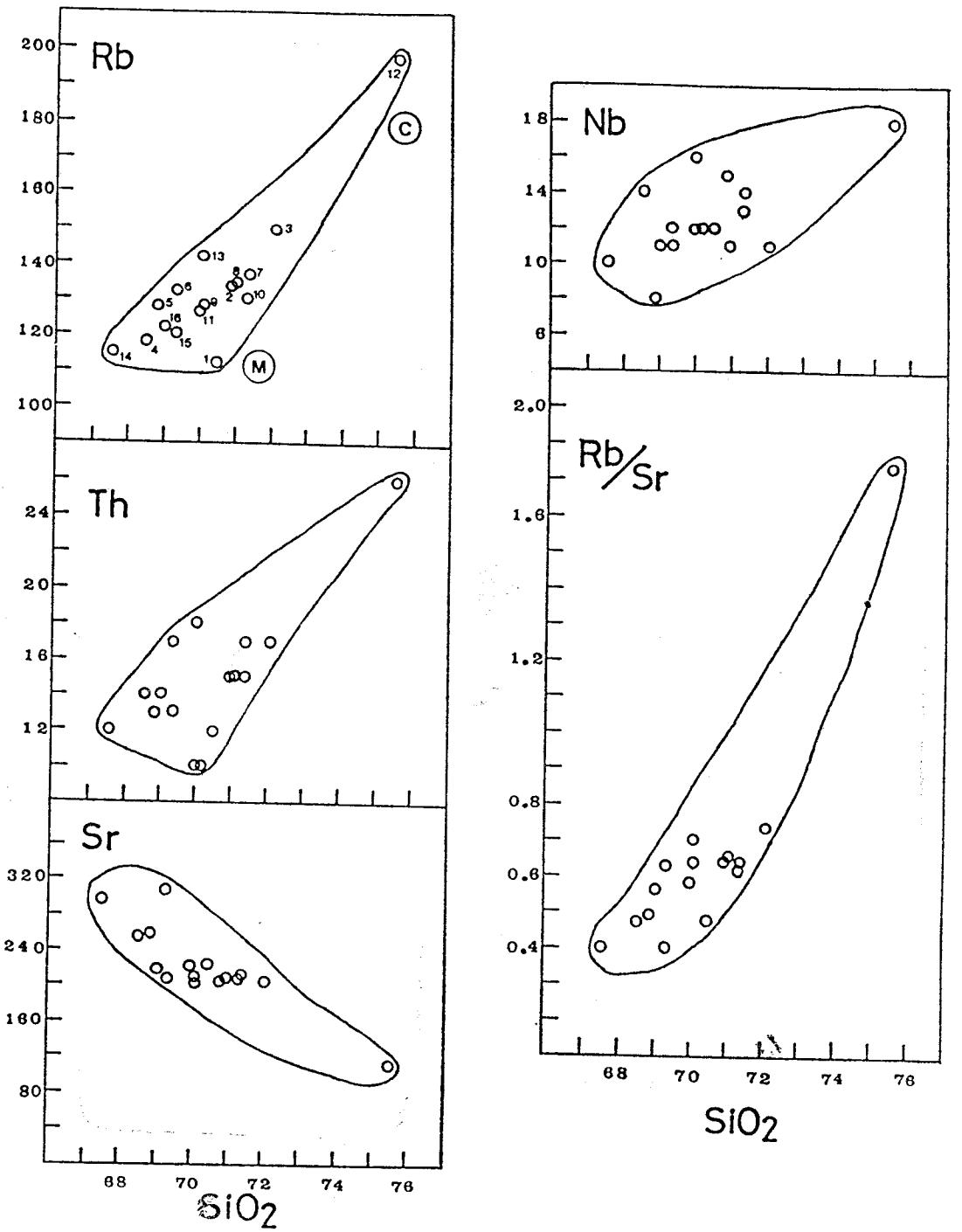

Fig. 7 Harker Variation diagrams (trace elements in ppm) for the Cretaceous Palgongsan granite. Sample numbers are as in Fig. 1.

The K/Rb ratios are plotted against the Differentiation Index to show a slightly negative trend (Fig. 8). It appears that both K and Rb were enriched at nearly constant rates during fractionation. The relationship between K_2O and Rb presents a good positive trend (Fig. 9), which

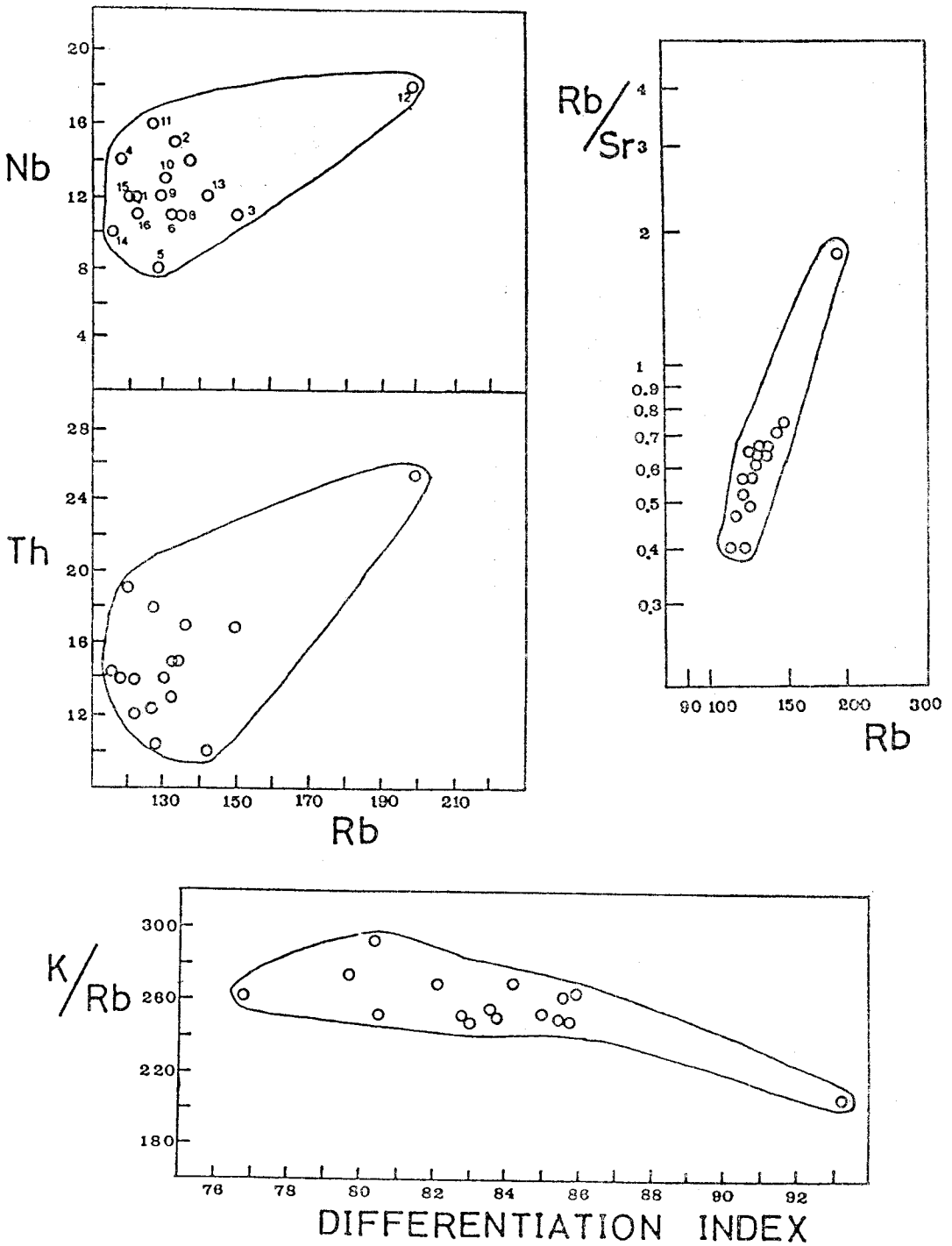

Fig. 8 Inter-element diagrams of trace elements (in ppm) for the Cretaceous Palgongsan granite.

occupies K_2O/Rb value of 250–350. The Rb/Sr ratios are plotted against Rb contents which illustrate a positive trend (Fig. 8). The Rb and Sr data plot in a well defined linear field showing negative correlation (Fig. 9), indicating that the variation could be dominated by feldspare fractionation.

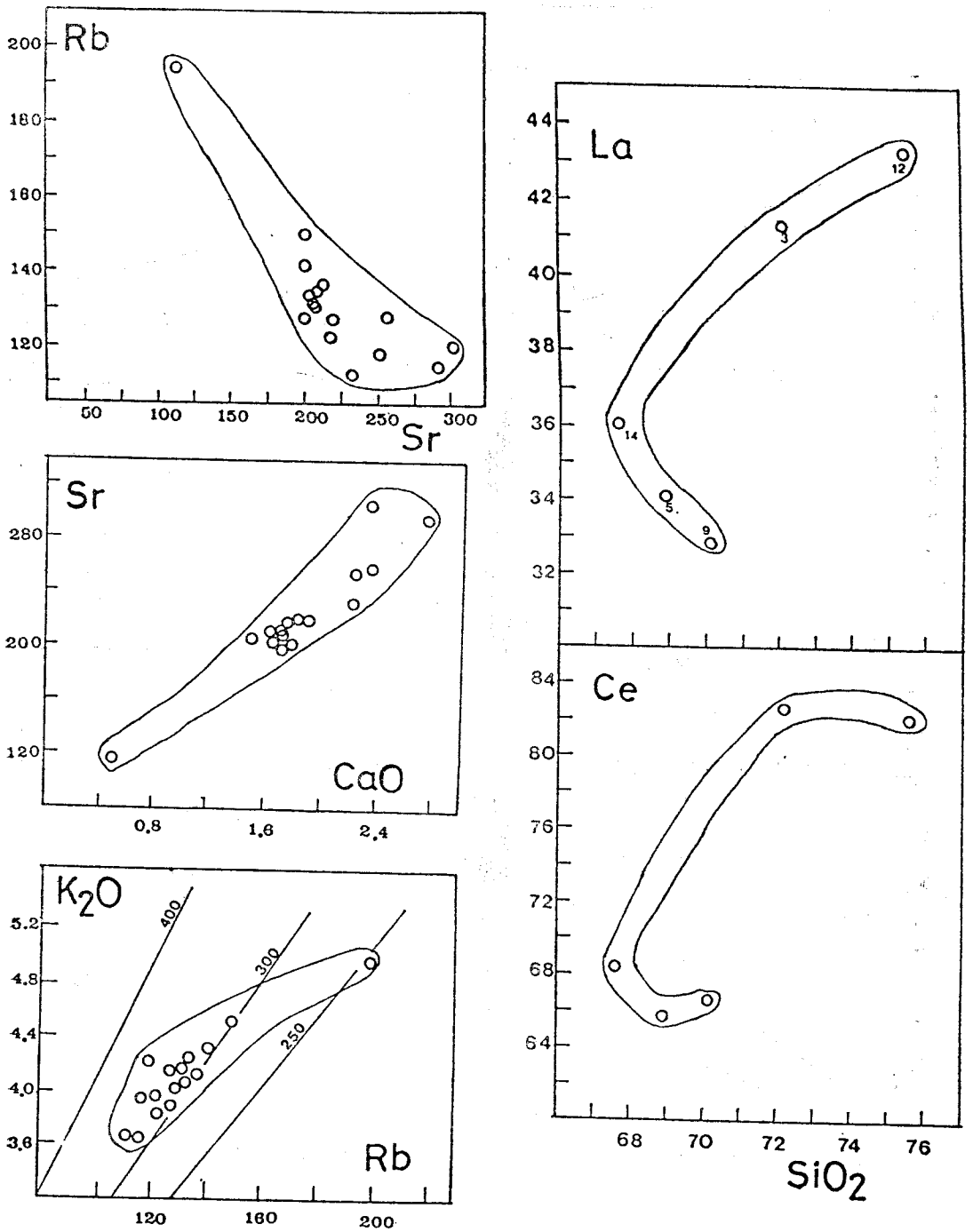

Fig. 9 Inter-element diagrams of trace elements (in ppm) for the Palgongsan granite.

Nb contents in the Palgongsan granite range from 11ppm in the margin to 18ppm in the centre of the pluton (mean value of 12.8 ± 2.4ppm), which illustrates a positive trend with SiO_2 (Fig. 7). Fig. 8 shows a positive relationship between Nb and Rb. The concentrations of Th range from 10ppm to 26ppm (average of 15 ± 4ppm). The plots of Th–SiO_2 and Th–Rb show positive cor-

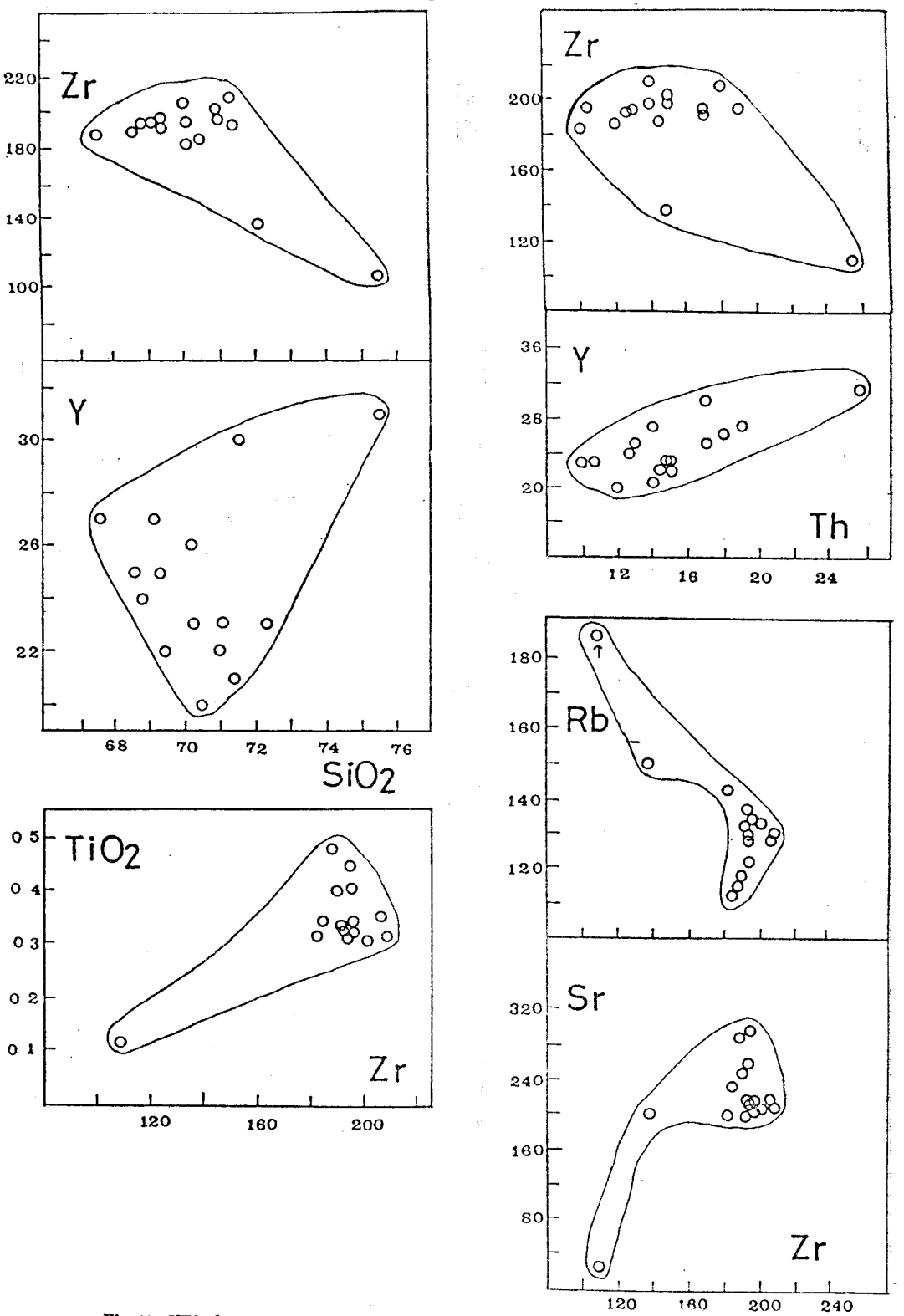

Fig. 10 HFS element and Y inter-element relationships for the Cretaceous Palgongsan granite.

Table 4. Rare-Earth Elements analyses (in ppm) of the Cretaceous Palgongsan granite

	CP. 3	CP. 5	CP. 9	CP. 12	CP. 14	$\bar{X}$	S
La	41.33	34.11	32.85	43.30	36,08	37.53	4.57
Ce	82.69	65.65	66.62	82.11	68.43	73.10	8.55
Nd	30.67	23.18	21.74	28.07	25.85	25.90	3.61
Sm	4.26	4.45	3.98	4.48	4.35	4.30	0.20
Eu	0.63	0.93	0.71	0.22	0.89	0.68	0.28
Gd	3.45	3.17	3.04	2.07	3.58	3.06	0.59
Tb	1.03	0.60	0.68	1.05	0.76	0.82	0.21
Tm	0.37	0.40	0.39	0.62	0.38	0.43	0.11
Yb	2.18	2.57	2.56	3.63	2.52	2.69	0.55
Lu	0.28	0.42	0.28	0.53	0.30	0.36	0.11
Hf	4.14	3.10	5.86	3.90	4.97	4.39	1.06
Ta	1.11	1.26	1.22	2.04	1.22	1.37	0.38
ΣREE	166.89	135.48	132.85	166.08	143.14	148.89	16.51
La/Yb	18.96	13.27	12.83	11.93	14.32	14.26	2.76
Ce/Yb	37.93	25.54	26.02	22.62	22.15	27.85	5.88
Eu/Eu*	0.51	0.75	0.62	0.24	0.61	0.55	0.19
(La/Sm)N	5.90	4.64	5.13	6.50	5.12	5.46	0.75
(Ce/Yb)N	9.50	6.44	6.79	5.78	6.96	7.09	1.42
(La/Yb)N	12.40	8.49	8.93	7.88	9.57	9.45	1.76
Zr/Hf	33	63	33	28	38	39	14
La/Ta	37	27	27	21	30	28	6
ΣCe	159.58	128.32	125.90	158.18	135.60	141.52	16.26
ΣY	7.31	7.16	6.95	7.90	7.54	7.37	0.37

∑REE: total concentration of REE
EU* : Eu value derived by interpolation between Sm and Gd
N : chondrite normalised value
∑Ce : sum of light REE (La to Eu)
∑Y : sum of heavy REE (Gd to Lu)

relations which are shown in Fig. 7 and Fig. 8, respectively. La contents in the Palgongsan granite range form 32.85ppm, in the margin, to 43.30ppm, in the centre of the pluton (mean of 37.53 ± 4.57 ppm), which show a positive trend with SiO_2 (Fig. 9).

Ce content range form 66.62ppm to 82.69ppm, with average of 73.1±8.55ppm.

HFS elements, REE, and Y

Zr contents are, generally higher in the margin than the central part of the pluton (mean value of 185 ± 26ppm). Zr shows negative correlations with SiO_2, Th and Rb, and presents positive relarionships with TiO_2 and Sr (Fig. 10). K/Zr ratios are high in the core part (380) relative to the chilled margin (156) of the Palgongsan granite, with average ratio of 191 ± 57. A plot of Y versus Zr (Fig. 10) serves to distinguish between fractional crystallisation and partial melting processes in the petrogenesis of igneous rocks (Tarney et al, 1977). The Zr/Y ratio changes only very slightly during fractional crystallisation, but the differences in partition coefficient between the two become significant during moderate to low degrees of partial melting, with Y being pro-

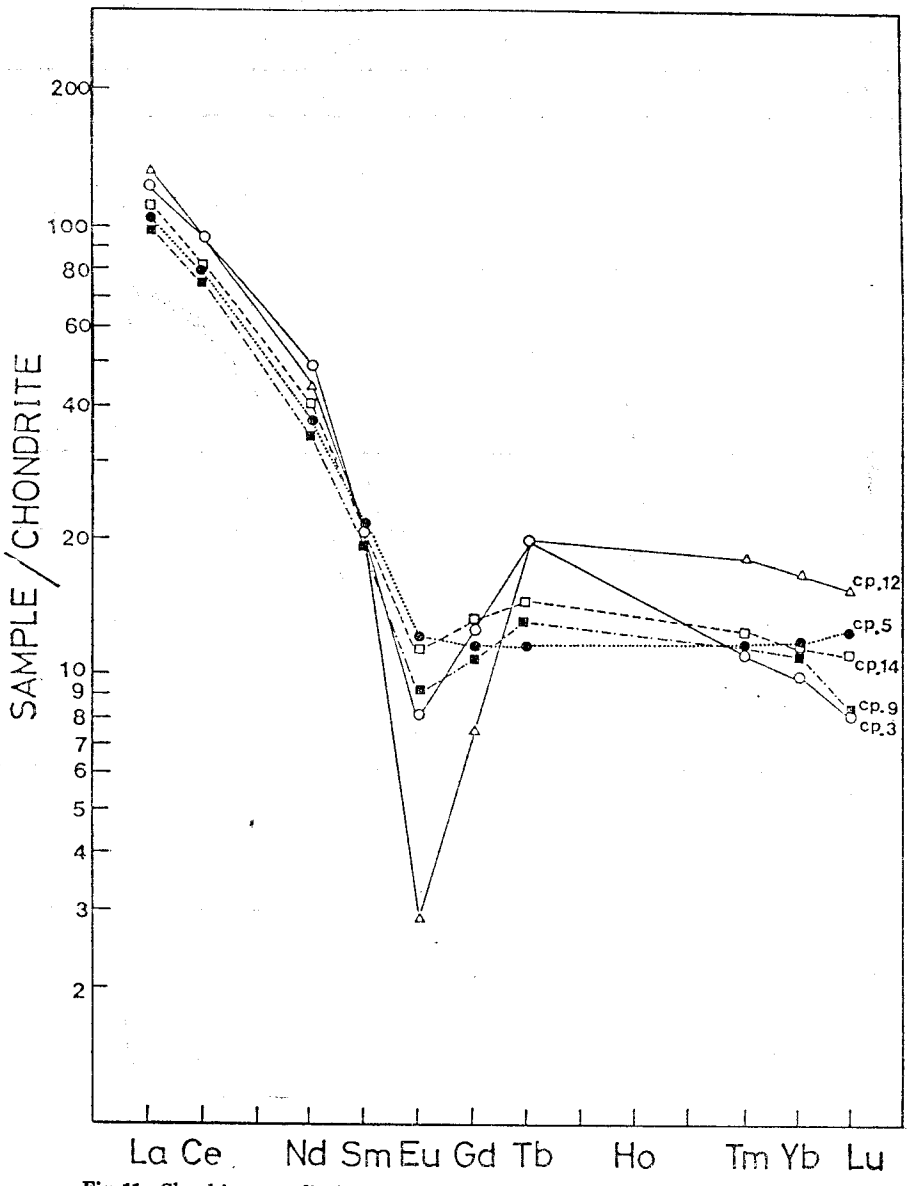

Fig. 11 Chondrite-normalised REE abundancess in the Cretaceous Palgongsan granite.

gressively ratained in the source at lower degrees of partial melting (Tarney & Saunders, 1979). It can be seen that the Palgongsan granite samples have generally constant Zr/Y ratios (mean of 7.71 ± 1.54), suggesting fractional crystallisation. Nb contents generally increase form the margins inward (average of 12.8 ± 2.4ppm).

Rare-earth elements (REE) were determined on 5 representative samples and the analytical results are presented in Table 4. The REE abundance data for these samples have been normalised to the average chondritic abundances (Frey et al., 1968), and plotted on a logarithmic scale against atomic number (Fig. 11).

Zr/Hf and La/Ta ratios are higher in the margin relative to the centre of the pluton (Table 4). The Palgongsan granite shows light REE enrichment and heavy REE depletion with $(Ce/Yb)_N$ ratios of 5.78–9.50 (the average ratio being 7.09 ±1.42). All the REE patterns in the studied

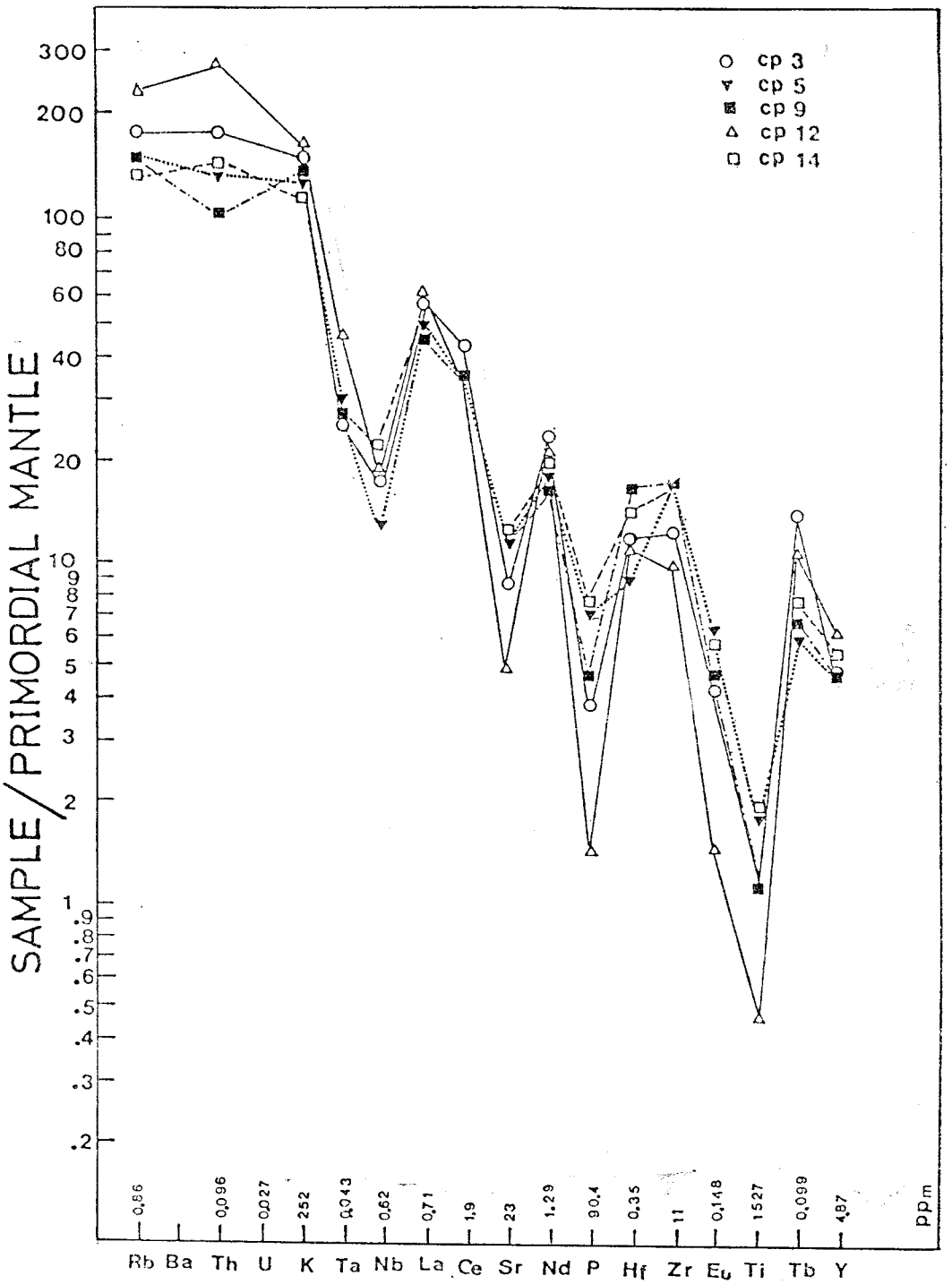

Fig. 12 Incompatible element abundances in the Palgongsan granite normalised to estimated primordial mantle abundances (Shaw, 1972).

granite have Eu negative anomalies with Eu/Eu* =0.24–0.75 (mean Eu/Eu* = 0.55). The Eu negative anomalies increase from the margin (Eu/Eu* = 0.75) to the central part (Eu/Eu* = 0.24) of the pluton. The negative Eu anomalies and gradual change of Eu/Eu* values through the Palgongsan granite, indicate the influence of feldspar fractionation.

The central part of the granite has undergone much stronger feldspar fractionation than the margin. Plagioclase has high phenocryst-matrix partition coefficients for Sr and Eu^{+2} and high K/Rb ratios (Arth, 1976).

The abundances of incompatible elements in the Palgongsan granite, normalised to an estimated undepleted primordial mantle composition (Shaw, 1972), are shown in Fig. 12. The left to right order of the element approximates to the decreasing bulk distribution coefficients (D values) between granitic liquid and mineral phases. The plot reveals that the Palgongsan granite is characterised by strong enrichment of Rb, Th, K, La, Ce, Nd, Hf, Zr and Tb relative to Ta, Nb, Sr, P and Ti. This is typical for calc-alkaline granitoid rocks.

Compatible elements

The Cr contents in the Palgongsan granite range from 4ppm to 15ppm (mean of 8.5 ± 3ppm). The concentration of Cr is generally higher in in the margin relative to the centre of the pluton. The Ni concentrations range form 1ppm to 5ppm (average value of 3.5 ± 1ppm). The plot between Ni and SiO_2 shows a negative trend. The V contents show a rather scattered negative correlation with SiO_2, and the concentrations of V is very high in the margin (37–44ppm) but lower in the centre (N.D.–19ppm). For equivalent values of Cr, Ni and V concentrations for the Palgongsan granite decrease consistently from margin to centre of the pluton, which reflects the inward increase in the effects of fractional crystallisation.

7. Mineral geochemistry

The varied mineralogical assemblages described petrogaphically in previous sections are here further defined in terms of chemical compositions and chemically determined crystallisation history. Alkali-feldspar, plagioclase and biotite from the 7 representative Palgongsan granite samples were studied, using the energy dispersive electron microprobe at the Department of Earth Sciences, University of Cambridge. Analytical method employed in this work, and accuracy and precision of analysis can be sent by the authour upon request. No published works are available on the mineral geochemistry of the Palgongsan granite.

Chemistry of alkali-feldspar and two-feldspar geothermometry

The alkali-feldspar in the Palgongsan granite shows perthitic texture, as described previously. The exsolution lamellae make estimation of original bulk compositions difficult. The analyses given in Table 5 are microprobe analyses of exsolved grains. The number of cations K^+ in alkali-feldspar and cations Na^+ in the perthite, generally increase from the margins inward. Perthitic alkali-feldspars yield some useful temperatures (Barth, 1962, 1968; Stormer & Whitney, 1977; Powell & Powell, 1977; Ferry, 1978; Brown & Parson, 1981), and of particular interest are temperature differences between the centre and the margin of the Palgongsan granite. The theoretical background of two-feldspar geothermometer is reviewed by Powell (1978). Analytical results of perthitic alkali-feldspars from the Palgongsan pluton are plotted on the graphical geothermometer (Powell 1978) in Fig. 13, which illustrates that the temperature of cessation of exsolution in perthitic alkali-feldspars was about 500–700°C at an assumed pressure of 2 Kbar. This graphic geothermometer shows that the perthites plot in a scattered range of temperature

Table 5. Electron microprobe analyses of perthitic alkali-feldspar in the Cretaceous Palgongsan granite

	CP. 2		CP. 4		CP. 5		CP. 8		CP. 11		CP. 12		CP. 13	
	AF	PL	AF	PL	AF	PL	AF	PL	AF	PL	AF	PL	AF	PL
SiO_2	67.154	63.197	66.532	62.641	65.456	64.770	65.340	63.560	66.072	63.628	66.477	64.867	66.383	63.887
Al_2O_3	18.279	22.972	19.034	23.410	18.792	22.239	18.066	22.475	18.954	22.711	18.294	21.677	18.585	22.756
FeO(t)	0.113	0.153	0.192	0.179	—	—	0.183	0.246	0.127	—	—	—	—	0.182
CaO	—	4.259	0.152	4.596	—	3.489	—	4.247	0.114	4.336	—	2.909	0.166	4.215
BaO	—	—	0.439	—	0.454	—	0.502	—	0.284	—	—	—	0.401	—
Na_2O	3.315	8.843	4.766	8.944	2.763	9.507	2.272	8.753	5.469	9.016	1.562	20.248	4.457	8.869
K_2O	10.599	0.442	8.742	0.202	12.370	0.341	12.891	0.632	8.548	0.199	14.594	10.308	10.080	0.674
Tota	99.460	99.866	98.857	99.972	99.835	100.346	99.254	99.913	99.568	99.890	100.928	100.009	100.072	100.584
Recalculated on 8 oxygens														
Si	3.050	2.800	3.000	2.776	2.994	2.846	3.014	2.817	2.990	2.813	3.019	2.862	3.005	2.813
Al	0.976	1.200	1.012	1.223	1.013	1.152	0.983	1.174	1.011	1.184	0.980	1.128	0.992	1.181
Fe	0.004	0.006	0.007	0.007	—	—	0.007	0.009	0.005	—	—	—	—	0.007
Ca	—	0.202	0.007	0.218	—	0.164	—	0.202	0.006	0.205	—	0.138	0.008	0.199
Ba	—	—	0.008	—	0.008	—	0.009	—	0.005	—	—	—	0.007	—
Na	0.291	0.759	0.417	0.768	0.245	0.810	0.203	0.752	0.480	0.773	0.138	0.877	0.391	0.757
K	0.612	0.025	0.503	0.011	0.722	0.019	0.759	0.036	0.494	0.011	0.846	0.017	0.582	0.038

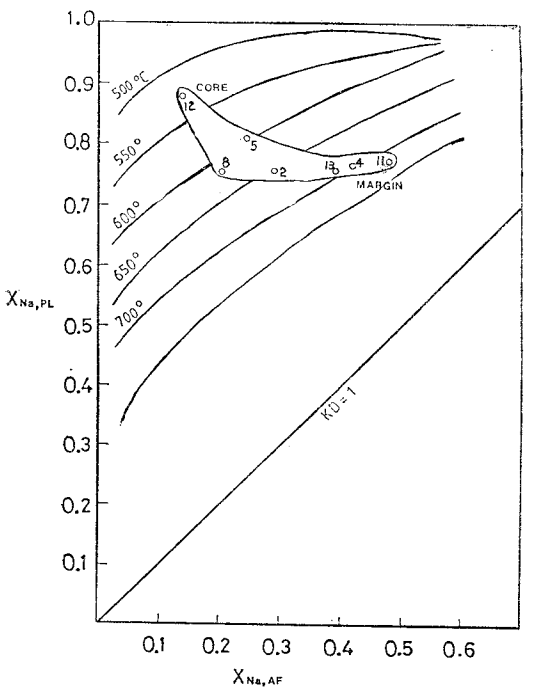

Fig. 13 Coexisting alkali feldspar-plagioclase geothermometer diagram at pressure of 2 Kbar.

over the Palgongsan granite as a whole, with low T at the core, and high T at the margin. Using Powell & Powell's geothermometer equation, calculated temperatures for cessation of exsolution remain also within a large range (about 500–700°C) when a range of pressures is considered (see Table 6). The temperatures of exsolution generally decrease form margin to core within the pluton. From these geothermometers, it can be concluded that the temperatures of exsolution in perthitic alkali-feldspars show a large variation, which illustrates that the Palgongsan granite crystallised form margin to core with about 200°C temperature difference between them. Comprehensive microprobe investigation of all cations present shows a progressive chemical evolution from the margin to the central part of the Palgongsan granite

Chemistry of plagioclase

Plagioclases from the Palgongsan granite occur as subhedral columnar plates which show parallel twinning. The plagioclase analytical results are presented in Table 7. The number of alkali ($X_{Na} + X_K$) cations in plagioclase increases from

Table 6. Temperatures of cessation of exsolution at the various pressures for the Cretaceous Palgongsan granite

	Mineral	X_{Na}	X_K	T°C				
				1Kb	3Kb	5Kb	7Kb	10Kb
CP. 2	AF	0.291	0.612	465	486	507	529	561
	PL	0.759	0.025					
CP. 4	AF	0.417	0.503	587	612	637	661	698
	PL	0.768	0.011					
CP. 5	AF	0.245	0.722	531	555	578	601	636
	PL	0.810	0.019					
CP. 8	AF	0.203	0.759	516	539	562	585	619
	PL	0.752	0.036					
CP. 11	AF	0.480	0.494	721	750	779	807	850
	PL	0.773	0.011					
CP. 12	AF	0.138	0.846	439	459	480	502	531
	PL	0.877	0.017					
CP. 13	AF	0.391	0.582	675	702	729	757	798
	PL	0.757	0.038					

$$T(K)=\frac{-X^2_{K(AF)}[6330+0.093P+2X_{Na(AF)}(1340+0.019P)]}{RlnKD+X^2_{K(AF)}[-4.63+1.54X_{Na(AF)}]}$$

$R=1.9872$ Cal

$$KD=\frac{X_{Na(AF)}}{X_{Na(PL)}}$$

(after Powell & Powell 1977)

the margin to the core part of the pluton, which illustrates a positive correlation with cation Si_2 (Fig. 14). However, the number of cation Ca^{++} in plagioclase generally decreases from the margins inward (Fig. 14). The chemistry of plagioclase reflects that plagioclase crystallised form the margin (high cation Ca^{++} and low alkali-cations) to the central part of the pluton.

Chemistry of biotite

Chemical considerations of biotite are limited by the inability of the electron microprobe to give separate values for Fe_2O_3, and the absence of data for Li_2O, F, Cl, and water. Owing to the above constratints, the purpose here is primarily to find the chemical variances of the biotites throughout the Palgongsan granite. Major element concentrations and structural formulae of biotites are given in Table 8. The Al_2O_3-total iron-MgO diagram shows that MgO and total iron contents vary considerably, whilst Al_2O_3 concentrations show little variation. The contents of MgO decrease from the margin to the central part of the pluton. Ionic Mg/(Mg + Fe) for biotites decrease from 65.04 to 34.57 as SiO_2 content of the whole-rock increase form 68.52 to 75.55 weight percent, which largely depends upon the presence and absence of an early crystallisation of opaque minerals (e.g. magnetite) from granitic magma. And in other words, an early uptake of magnetite from the granitic magma is followed by the decrease of Mg/(Mg + Fe) for mafic silicates as the differentiation of the magma proceeds.

Table 7. Plagioclase analyses for the Palgongsan granite

	CP. 2	CP. 4	CP. 5	CP. 8	CP. 11	CP. 12	CP. 13
SiO_2	63.041	63.695	62.842	63.244	63.217	64.951	63.936
Al_2O_3	23.122	22.614	23.046	22.717	22.748	21.394	22.055
FeO(t)	0.164	0.196	—	0.168	0.245	0.132	—
CaO	4.621	3.880	4.408	4.172	4.345	2.050	3.272
Na_2O	8.969	9.043	8.528	9.176	9.191	10.342	9.767
K_2O	0.564	0.450	0.649	0.580	0.344	0.305	0.548
Total	100.481	99.869	99.473	100.058	100.09	99.174	99.578
Recalculated on 8 oxygens							
Si	2.785	2.819	2.795	2.803	2.800	2.877	2.839
Al	1.204	1.180	1.209	1.187	1.188	1.128	1.154
Fe	0.006	0.007	—	0.006	0.009	0.005	—
Ca	0.219	0.184	0.210	0.198	0.260	0.097	0.156
Na	0.768	0.776	0.735	0.788	0.789	0.888	0.841
K	0.032	0.025	0.037	0.033	0.019	0.017	0.031
Mole proportion (%)							
Or	3.1	2.5	3.8	3.3	1.9	1.7	3.0
Ab	75.4	78.8	74.8	77.3	77.8	88.6	81.8
An	21.5	18.7	21.4	19.4	20.3	9.7	15.2

Table 8. Analyses of bioties from the Palgongsan granite

	CP. 2	CP. 4	CP. 5	CP. 8	CP. 11	CP. 12	CP. 13	CP. 15
SiO_2	38.015	38.985	37.494	37.391	36.397	37.437	38.343	38.038
Al_2O_3	11.929	12.656	13.026	12.019	12.298	11.457	12.584	13.140
TiO_2	4.240	4.814	4.953	4.975	4.651	2.987	4.934	5.165
FeO(t)	17.619	15.412	17.700	14.266	20.884	25.016	16.682	16.820
MgO	13.327	14.359	12.795	14.891	10.553	7.417	13.840	13.355
MnO	0.201	—	0.169	0.188	0.505	1.228	0.262	—
CaO	—	—	0.128	—	0.100	—	—	—
K_2O	9.375	9.625	9.203	9.449	9.012	9.182	9.322	9.423
Total	94.707	95.854	95.468	93.178	94.40	94.725	95.966	95.941
Recalculated on 11 oxygens								
Si	2.899	2.897	2.835	2.860	2.839	2.973	2.867	2.845
Al	1.072	1.109	1.161	1.084	1.131	1.073	1.109	1.159
Ti	0.243	0.269	0.282	0.286	0.273	0.178	0.277	0.291
Fe	1.124	0.958	1.119	0.912	1.362	1.662	1.043	1.052
Mg	1.515	1.590	1.442	1.697	1.227	0.878	1.542	1.489
Mn	0.013	—	0.011	0.012	0.033	0.083	0.017	—
Ca	—	—	0.010	—	0.008	—	—	—
K	0.912	0.913	0.888	0.922	0.897	0.930	0.889	0.899
Ionic Mg/(Mg+Fe)	57.41	62.41	56.30	65.04	47.38	34.57	59.65	58.59

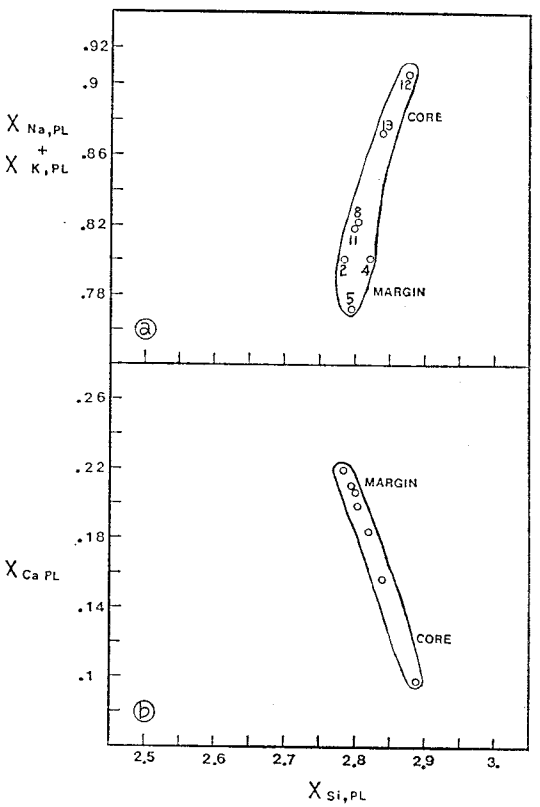

M : margin of the pluton
C : core of the pluton

Fig. 14 Inter-element variations between cations alkali and silica, and cations Ca and Si in plagioclase.

8. Discussion and conclusions

The Palgonsan granite is a concentric texturally and compositionally zoned pluton. The granite is progressively more felsic inword. The structural relationship between the granitic intrusion and joint pattern (N50°–70°W dominant) suggests that the intrusion process allowed the roof to break up into rectangular blocks along previously established lines of weakness, joints and vertical faults. The granite ranges in composition form intermediate to acid, and produce a smooth calc-alkaline trend on an AFM diagram. The smooth consistent trends of the major and trace elements within the pluton can best be explained by fractional crystallisation. There is an initial Fe-enrichment until both Ti and Mg decrease sharply with titanomagnetite crystallisation. Phosphorous also increases until apatite separates, while Sr consistently decreases because of early and continued plagioclase crystallisation. Other incompatible elements, such as Rb, Th and Nb, increase progressively with fractionation. Total REE levels increase with fractionation, and with the eventual development of distinct negative Eu anomalies ($Eu/Eu^* = 0.75–0.24$) in the Palgongsan granite. The behaviour of the rare-earth elements is that the general increase in REE concentrations with the gradual development of negative Eu anomalies in more silicic compositions seen in the Andean and East Greenland calc-alkaline plutons (see Tarney & Saunders, 1979). Rb/Sr and K can be attributed to the effects of fractional crystallisation dominated by the removal of plagioclase. Zr/Y ratios do reduce with fractionation, especially in the more silicic compositions (e.g. central part of the pluton), indicating partitioning of REE into the major mineral phases as the magma becomes more silicic. Notable is the strong coherence during fractionation of SiO_2, K_2O, Rb, Th, Nb, La, Ce and REE.

Major and trace element variations are consistent with a modal of inward fractionational crystallisation of parental basic magma. There are abundant well-digeted andesitic xenoliths in the marginal part of the pluton. The concentrations of high HFS and low LIL elements in the Palgongsan granite also support the conclusion that the granite derived form fractionation of igneous parent magma ("I-type" granite).

The compositional zoning in the Palgongsan granite indicates that, with decreasing temperature, the sequence solidified from the margins inward. The compositional zoning resulted from crystal fractionation that could have involved a fairly simple mechanism of differentiation "in situ", such as (1) preferential accretion of crystalline

material present in the magma to the margins of the magma chamber, thus displacing the melt phase progressively inward; and/or (2) downward setting of crystals, problably accompanied by upward movement of melt and volatiles.

The observations and arguments presented for the Palgongsan granite lead to the following general conclusions;

1. The granite is a calc-alkaline subsolvus monzogranite. It is generally a medium grained granite, which consists of quartz, feldspars biotite and hornblende. The grain size of the pluton increases form its margins inwards;
2. Many of the major and trace element characteristics of the Palgongsan granite are consistent with a relationship by fractional crystallisation to form a chemically zoned pattern;
3. The granite shows light REE enrichment with (Ce/Yb)N ratios of 5.78-9.50. All the REE patterns show Eu negative anomalies which bceome larger from the margin (Eu/Eu^* = 0.75) to the core (Eu/Eu^* = 0.24) of the pluton, mainly due to feldspar fractionation;
4. Mineral geochemistry studies also show the zonal structure of the Palgongsan granite. The two-feldspar geothermometer shows that the temperature difference between the margin and the core part of the pluton is about 200°C at various assumed pressures;
5. The Palgongsan granite shows characteristics of "I-type" granite by mineralogy and chemical composition (Chappell & White, 1974) and "magnetite"-series (Ishihara, 1977).

Acknowledgements

I would like to acknowledge the invaluable help given by Dr. P. H. Banham in univ. of London. In particular, thanks are extended to Dr. G.F. Marriner for the help of XRF and INAA, and to Dr. P.J. Treloar for the use of EPMA in Univ. of Cambridge. Sincere thanks are expressed to Dr. A.D Saunders and Prof. G.C. Brown for useful discussion on geochemical behaviour of trace element and data processing.

References

Arth, J.G. (1976), Behaviour of trace elements during magmatic processes-a summary of theoretical models and their applications. J. of Reserach of the U.S. geological survey, 4, 41-47.

Bailey, E.H. & Stevens, R.N. (1960), Selective staining of K-feldspar and plagioclase on rock slabs and thin sections. Am. Mineralogist, 45, 1020-1025.

Barth, T.F.W. (1962), A final proposal for calculation the mesonorm of metamorphic rocks. J. Geol., 70, 494-498.

Barth, T.F.W. (1968), Additional data for the two-feldspar geothermometer. Lithos, I, 305-306.

Brown, W. L. & Parsons, I. (1981), Torwards a more practical two-feldspar geothermometer. Contr. Min. petrol., 76, 369-377

Chang, K. H. (1975), Cretaceous stratigraphy, sedimentation and tectonics of southeastern Korea. J. Geol. Soc. Korea, 13, 76-90.

Chang, K.H. (1978), Aspects of Mesozoic and Cenozoic tectonic history of Korea and related regions. J. Geol. Soc. Korea, 14 (2), 25-31.

Chappell, B.W. & White, A.J.R. (1974), Two contrasting granite types. Pacific geology, 8, 173-174.

Chayes, F. & Metais, D. (1963), On the relation between suites of CIPW and Barth-Niggli norms. Carnegie Inst. Washtn. Year Book, 193.

Choi, H.I. (1979), Cretaceous fluvio-lacustrine sediments in the southeastern part of the Gyeongsang sedimentary basin in Korea. Geol. Soc. China, Mem., 3, 195-218.

Cox, K.G., Bell, J.D. & Pankhurst, R.J. (1979), The interpretation of igneous rocks. George Allen & Unwin, 450pp.

Ferry, J.M. (1978), Fluid interaction between granite

and sediment during metamorphism, south-central Maine, Am. J. Sci., 278, 1025-1056.

Frey, F.A., Haskin, M., Poetz, J. & Haskin, L., (1968), Rare-earth abundaneces in basic rocks, J. of Geophysical Research, 73, 6085-6098.

Geol. Min. Inst. Korea (1973), 1:250,000 Geological map of Korea. GMIK, Seoul, Korea

Hanson, G.N. (1978), The application of trace element to the petrogenesis of igneous rocks of granitic composition. Earth. Plan. Sci. Lett., 38, 26-43.

Ishihara, S. (1977), The magnetite-series and ilmenite-series granitic rocks. Mining Geol., 27, 293-305.

Jin, M.S., Kim, S.Y. & Lee, J.S. (1981), Granitic magmatism and associated mineralization in the Gyeongsang Basin, Korea. Mining Geol., 31, 245-260.

Kim, O.J. (1971), Study on the intrusion epochs of younger granites and their bearing to orogenies of South Korea. J. Kor. Inst. Min. Geol., 4, 1-9.

Kobayashi & Suzuki (1937), Non-marine shells of Nagdong-Wakino series. Japan.J. Geology & Geography, 14, 1-2.

Larsen, E.S. (1948), Batholith and associated rocks of Corona, Elsinore and San Luis key quadrangles, Southern California. Mem. Geol. Soc. Am., 29, 182pp.

Lee, S.M. (1974), A relative study on plutonism and mineralization in Korea. Ministry of Science & Techonlogy, R-74-48.

Petro, W.L., Vogel, T.A., Wilband, J.T. (1979), Major element chemistry of plutonic rocks/ suites from compressional and extensional plate boundaries. Chemical geology, 26, 217-235.

Powell, M. (1978), The crystallisation history of the Igdlerfigssalik nepheline syenite intrusion, Greenland. Lithos, 11, 99-120.

Powell, M. & Powell, R. (1977), Plagioclase-alkali feldspar geothermometry revisited. Mineral Mag., 41, 253-256.

Shaw, D.M. (1972), Development of the early continental crust, I. Use of trace element distribution coefficient models for the protoarchean crust. Can. J. Earth Sci., 9, 1577-1595.

Schilling, J.G. (1973), Iceland mantle plume: geochemical evidence along Reykjanes Ridge. Nature, 242, 565-571.

Stephens, W.E. & Halliday, A.N. (1979), Compositional variation in the Galloway plutons. In: Atherton, M.P. & Tarney, J. (eds), Origin of granite batholiths, geochemical evidence. Shiva Publ. Ltd., 9-17.

Stormer, J.C. (Jr), (1975), A practical two-feldspar geothermometer. Am. Mineral., 60, 667-674.

Stormer, J.C. (Jr) & Whitney, J.A. (1977), Two-feldspar geothermometry in granulite facies metamorphic rocks. Contrib. Mineral Petrol., 65, 123-133.

Streckeisen, A. (1976), To each plutonic rocks its proper name, Earth. Sci. Rev., 12, 1-33.

Tarney, J. & Saunders, A.D. (1979), Trace element constraints on the origin of Cordilleran Batholiths. In: Atherton, M.P. & Tarney, J. (eds), Origin of granite batholiths, geochemical evidence. Shiva Publ. Ltd, 90-105.

Tarney, J. & Windley, B.F. (1977), Chemistry, thermal gradients and evolution of the lower continental crust. J.Geol. Soc. London, 134, 153-172.

Tateiwa, I. (1929), Geological Atlas of Korea. No. 10, Gyeongiu, Yoocheon, Daegu and Waegwan Sheets. Geol. Surv. Chosen (Korea).

Thornton, C.P. & Tuttle, O.F. (1960), Chemistry of igneous rocks. I; Differentiation index. Am. J. Sci., 258, 664-684.

Tuttle, O.F. & Bowen, N.L. (1958), Origin of grnite in the light of experimental studies in the studies in the system $NaAlSi_3O_8$-$KAlSi_3O_8$-SiO_2-H_2O. Geol. soc. Am. Memoir, 74.

Wilson, A.D. (1955), A new method for the determination of ferrous iron in rocks and minerals. Bull. Geol. Surv. Great Britain, 9, 56-58.

Wright, J.B. (1969), A simple alkalinity ratio and its application to questions of non-orogenic granite genesis. Geol. Mag., 106, 370-384.

Yang, S.Y. (1976), On fossils form the Gyongsang group-especially on some of the Moluscan fauna. J. Geol. Soc. Korea, 12, 215-236.

Yang, S.Y. (1979), On the discovery of two new fossils form the Yeonhwadong Formation, the Gyeongsang group (Abstr). J. Geol. Soc. Korea. 15, 101-102.

白堊紀 八公山 花崗岩의 岩石學的 및 地球化學的 硏究

洪 永 國*

要約 : 八公山 花崗岩은 칼크—알카라인 Subsolvus 몬조 花崗岩에 屬하고 中粒質이며, 石英, 長石, 黑雲母 및 각섬석으로 構成되어 있다. 花崗岩體의 鑛物粒子는 주변부에서 中心部로 갈수록 대체로 커지며 主構成元素 및 微量元素들도 帶狀分布를 보여주며 本花崗岩은 分別結晶作用에 依하여 形成되었다. 八公山 花崗岩의 (Ce/Yb)N 는 5..78–9.50 이며 LREE가 富化되어 있다. 全體的인 희토류元素分布는 Eu negative 異常値를 보여주며 Eu/Eu*는 岩體의 주변부(0.75)에서 中心部(0.24)로 갈수록 그 變化의 幅이 커지고 이는 主로 長石分結의 영향에 依한 것이다. 本 花崗岩體는 경장석, 사장석및 흑운모의 結果에서도 化學成分上 帶狀分布를 보여주며, 本岩體內 two-feldspar의 地質溫度計算結果는 주변부에서는 約 700°C (4 Kbar) 中心部에서에서 500°C(2 Kbar)各各 平衡安定 된것으로 나타났다. 本 八公山 花崗岩은 鑛物組成 및 化學成分(높은量의 HFS 원소 및 낮은量 LIL 원소)이 "I-type"에 屬하는 것으로 思料된다.

*동력 자원 연구소